Available online at www.sciencedirect.com
ScienceDirect
*Chinese Journal of Natural Medicines* 2021, **19**(9): 700-705
doi: 10.1016/S1875-5364(21)60088-2
Chinese Journal of Natural Medicines

•Research article•

# Biotransformation of *α*-asarone by *Alternaria longipes* CGMCC 3.2875

ZOU Jian[1, 4Δ], ZHANG Shuai[2Δ], ZHAO Huan[3], WANG Yong-Heng[1], ZHOU Zheng-Qun[1], CHEN Guo-Dong[1], HU Dan[1], LI Ning[2], YAO Xin-Sheng[1, 2], GAO Hao[1, 2*]

[1] *Institute of Traditional Chinese Medicine & Natural Products, College of Pharmacy/Guangdong Province Key Laboratory of Pharmacodynamic Constituents of TCM and New Drugs Research, Jinan University, Guangzhou 510632, China;*
[2] *College of Traditional Chinese Materia Medica, Shenyang Pharmaceutical University, Shenyang 110016, China;*
[3] *College of Traditional Chinese Medicine, Jinan University, Guangzhou 510632, China;*
[4] *Integrated Chinese and Western Medicine Postdoctoral Research Station, Jinan University, Guangzhou 510632, China*

Available online 20 Sep., 2021

**[ABSTRACT]** Biotransformation of *α*-asarone by *Alternaria longipes* CGMCC 3.2875 yielded two pairs of new neolignans, (+) (7*S*, 8*S*, 7′*S*, 8′*R*) *iso*-magnosalicin (**1a**)/(−) (7*R*, 8*R*, 7′*R*, 8′*S*) *iso*-magnosalicin (**1b**) and (+) (7*R*, 8*R*, 7′*S*, 8′*R*) magnosalicin (**2a**)/(−) (7*S*, 8*S*, 7′*R*, 8′*S*) magnosalicin (**2b**), and four known metabolites, (±) acoraminol A (**3**), (±) acoraminol B (**4**), asaraldehyde (**5**), and 2, 4, 5-trimethoxybenzoic acid (**6**). Their structures, including absolute configurations, were determined by extensive analysis of NMR spectra, X-ray crystallography, and quantum chemical ECD calculations. The cytotoxic activity and A$\beta_{42}$ aggregation inhibitory activity of all the compounds were evaluated. Compound **2** displayed significant anti-A$\beta_{42}$ aggregation activity with an inhibitory rate of 60.81% (the positive control EGCG: 69.17%). In addition, the biotransformation pathway of *α*-asarone by *Alternaria longipes* CGMCC 3.2875 was proposed.

**[KEY WORDS]** Biotransformation; *α*-Asarone; *Alternaria longipes* CGMCC 3.2875; Anti-A$\beta_{42}$ aggregation activity
**[CLC Number]** R284 **[Document code]** A **[Article ID]** 2095-6975(2021)09-0700-06

## Introduction

Biotransformation is a valuable method to transform one organic compound into its metabolites in bulk amounts with more specificity, which has been extensively utilized for structural modification and metabolism studies of bioactive compounds [1-4]. In particular, such a method has been applied for some famousl natural compounds to obtain diverse structures and more active compounds, such as artemisinin, paclitaxel, and protopanaxatriol [1].

*Acorus tatarinowii* Schott, belonging to the family Araceae, is a perennial herbaceous plant mainly distributed in China, Japan, and India. The rhizome of *A. tatarinowii* Schott has been used as a well-known traditional Chinese herb for the treatment of epilepsy, amnesia, chronic insomnia, tinnitus, and hearing loss [5]. *α*-Asarone is the major and representative ingredient isolated from the rhizome of *A. tatarinowii* Schott and exhibits a variety of biological activities such as antiepileptic, antidepressant, anxiolytic, neuroprotective, and hypolipidemic effects [6]. In our previous research on the chemical constituents of *A. tatarinowii* Schott, an abundance of *α*-asarone, some novel asarone derivatives, sesquiterpenoids, and nitrogenous compounds, were isolated [7-11]. In order to search for more diverse asarone derivatives, a biotransformation study of *α*-asarone was carried out. Twenty-four strains of fungi were used for preliminarily screening the microbial transformation of *α*-asarone. The results showed that *Alternaria longipes* CGMCC 3.2875 exhibited good capability to transform *α*-asarone. Further, six transformed products of *α*-asarone were isolated and identified, including two pairs

**[Received on]** 18-Jun.-2021
**[Research funding]** This work was supported by the National Key Research and Development Program of China (Nos. 2018YFA0903200 and 2018YFA0903201), the National Natural Science Foundation of China (Nos. 81925037 and 31900284), the Chang Jiang Scholars Program (Young Scholar) from the Ministry of Education of China (GAO Hao, 2017), the National High-level Personnel of Special Support Program (No. 2017RA2259), the Local Innovative and Research Teams Project of Guangdong Pearl River Talents Program (No. 2017BT01Y036), and K. C. Wong Education Foundation (GAO Hao, 2016).
[*] **Corresponding author]** E-mail: tghao@jnu.edu.cn
[Δ] These authors contributed equally to this work.
These authors have no conflict of interest to declare.
Dedicated to the 90th Anniversary of the Founding of Shenyang Pharmaceutical University

of new neolignans, (+) (7*S*, 8*S*, 7′*S*, 8′*R*) *iso*-magnosalicin (**1a**)/(−) (7*R*, 8*R*, 7′*R*, 8′*S*) *iso*-magnosalicin (**1b**) and (+) (7*R*, 8*R*, 7′*S*, 8′*R*) magnosalicin (**2a**)/(−) (7*S*, 8*S*, 7′*R*, 8′*S*) magnosalicin (**2b**), along with four known compounds, including (±) *ent*-acoraminol A (**3**), (±) acoraminol B (**4**), asaraldehyde (**5**), and 2, 4, 5-trimethoxybenzoic acid (**6**) (Fig. 1). Compounds **1**−**2** are a class of rare magnosalicin (7-*O*-8′/8-7′) type new neolignans. This is the first time that optically pure magnosalicin type neolignans are obtained from racemates, and their absolute configurations are established. In addition, the cytotoxicities and anti-A$\beta_{42}$ aggregation activities of all compounds were evaluated. Moreover, a plausible pathway of the metabolites of *α*-asarone transformed by *Alternaria longipes* CGMCC 3.2875 was proposed.

## Results and Discussion

Compound **1** was isolated as white powder. Its molecular formula $C_{24}H_{32}O_7$ (nine degrees of unsaturation) was determined by HR-ESI-MS at *m*/*z* 455.2039 $[M + Na]^+$ (Calcd. for $C_{24}H_{32}O_7Na$, 455.2046). The $^{13}C$ NMR spectrum showed 24 carbon signals, which was consistent with the deduction of the HR-ESI-MS. Combined with the DEPT 135 experiment, these carbons were categorized into eight $sp^2$ non-protonated carbons ($\delta_C$ 154.8, 153.5, 150.9, 149.8, 144.8, 144.1, 123.9, and 118.9), four $sp^2$ methine carbons ($\delta_C$ 117.2, 113.8, 99.7, and 99.5), four $sp^3$ methine carbons ($\delta_C$ 82.3, 80.4, 48.9, and 47.0), six methoxyl group carbons ($\delta_C$ 57.7, 57.6, 57.2, 56.9, 56.8, and 56.7), and two methyl carbons ($\delta_C$ 16.9 and 12.6). In the $^1H$ NMR spectrum of **1**, the characteristic protons for six methoxyl groups [$\delta_H$ 3.87 (s), 3.85 (s), 3.81 (s) × 2, 3.79 (s), and 3.78 (s)], two methyl groups [$\delta_H$ 1.14 (d, *J* = 6.5) and 0.65 (d, *J* = 6.8)], four aromatic protons [$\delta_H$ 7.01 (s), 6.96 (s), 6.71 (s), and 6.66 (s)], and four methine protons [$\delta_H$ 5.06 (d, *J* = 9.8 Hz), 4.79 (overlapped), 3.91 (dd, *J* = 6.5, 4.8), and 2.71 (ddq, *J* = 9.8, 6.8, 6.5 Hz)] were observed. The $^1H$ and $^{13}C$ NMR data of **1** (Tables 1−2) were nearly identical to those of magnosalicin, except that the chemical shifts for some of the resonances corresponding to the tetrahydrofuran ring. The detailed analysis of the $^1H$−$^1H$ COSY and HMBC data of **1** (Fig. 2) established the same planar structure as that of magnosalicin.

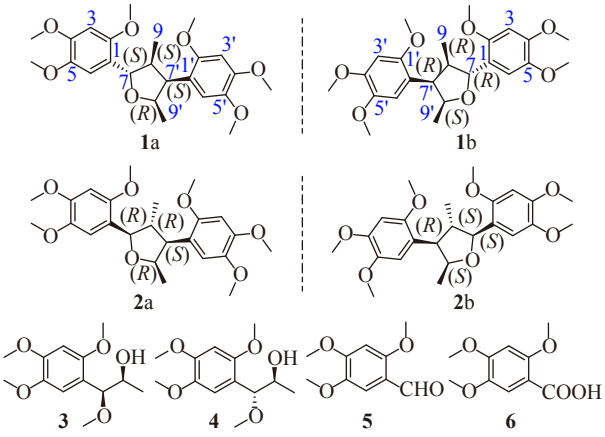


**Fig. 1 Structures of compounds 1−6**

**Table 1 $^1H$ NMR data (δ in ppm, *J* in Hz) for 1 ($CD_3OD$, 400 MHz) and 2 ($CDCl_3$, 300 MHz)**

| Position | 1 * | 2 * |
|---|---|---|
| 3 | 6.66, s | 6.53, s |
| 6 | 7.01, s | 7.13, s |
| 7 | 5.06, d (9.8) | 4.96, d (9.0) |
| 8 | 2.71, ddq (9.8, 6.8, 6.5) | 2.31, ddq (10.5, 9.0, 6.5) |
| 9 | 0.65, d (6.8) | 1.03, d (6.5) |
| 3′ | 6.71, s | 6.53, s |
| 6′ | 6.96, s | 6.68, s |
| 7′ | 3.91, dd (6.5, 4.8) | 3.59, dd (10.5, 8.5) |
| 8′ | 4.79 | 4.60, dq (8.5, 6.4) |
| 9′ | 1.14, d (6.5) | 0.89, d (6.4) |
| 2-$OCH_3$ | 3.78, s | 3.80, s |
| 4-$OCH_3$ | 3.85, s | 3.89, s |
| 5-$OCH_3$ | 3.81, s | 3.87, s |
| 2′-$OCH_3$ | 3.79, s | 3.81, s |
| 4′-$OCH_3$ | 3.87, s | 3.89, s |
| 5′-$OCH_3$ | 3.81, s | 3.78, s |

* Indiscernible signals owing to overlapping or having complex multiplicity are reported without designating multiplicity

**Table 2 $^{13}C$ NMR data (δ in ppm) for 1 ($CD_3OD$, 100 MHz) and 2 ($CDCl_3$, 75 MHz)**

| Position | 1 | 2 |
|---|---|---|
| 1 | 123.9, C | 121.5, C |
| 2 | 153.5, C | 151.7, C |
| 3 | 99.5, CH | 97.6, CH |
| 4 | 150.9, C | 148.8, C |
| 5 | 144.8, C | 143.3, C |
| 6 | 113.8, CH | 111.2, CH |
| 7 | 82.3, CH | 80.6, CH |
| 8 | 48.9, CH | 44.4, CH |
| 9 | 12.6, $CH_3$ | 14.9, $CH_3$ |
| 1′ | 118.9, C | 119.4, C |
| 2′ | 154.8, C | 152.2, C |
| 3′ | 99.7, CH | 97.3, CH |
| 4′ | 149.8, C | 148.0, C |
| 5′ | 144.1, C | 142.7, C |
| 6′ | 117.2, CH | 112.9, CH |
| 7′ | 47.0, CH | 49.3, CH |
| 8′ | 80.4, CH | 75.9, CH |
| 9′ | 16.9, $CH_3$ | 19.0, $CH_3$ |
| 2-$OCH_3$ | 57.7, $CH_3$ | 56.1, $CH_3$ |
| 4-$OCH_3$ | 56.8, $CH_3$ | 57.0, $CH_3$ |
| 5-$OCH_3$ | 56.9, $CH_3$ | 56.5, $CH_3$ |
| 2′-$OCH_3$ | 57.6, $CH_3$ | 56.1, $CH_3$ |
| 4′-$OCH_3$ | 56.7, $CH_3$ | 56.6, $CH_3$ |
| 5′-$OCH_3$ | 57.2, $CH_3$ | 56.3, $CH_3$ |

The relative configuration of **1** was determined by NOESY data (Fig. 3). The NOESY correlations between H-8 and H-8′, between H-8 and H-6, and between H-6 and H-8′ indicated that H-8, H-8′, and C-1 were on the same face of the tetrahydrofuran ring (7-*O*-8′). Furthermore, the NOESY correlations between H-6′ and H-7, between H-7 and $H_3$-9, and between H-6′ and $H_3$-9′ manifested that H-7, $H_3$-9, C-1′, and $H_3$-9′ were on the same face of the tetrahydrofuran ring adopting the opposite orientation as H-8. Thus, the relative configuration of **1** was designated as 7*S**, 8*S**, 7′*S**, 8′*R**, and named as *iso*-magnosalicin.

The NMR data of **2** was similar to *iso*-magnosalicin (**1**). Further detail NMR analyses involving $^1$H−$^1$H COSY and HMBC established the same planar structure as that of **1**. In the NOESY experiment (Fig. 3), the observed correlations between H-6 and H-8/H-9′, and between H-6′ and H-8/H-9′ demonstrated that C-1, H-8, H-9′, and C-1′ were on the same face of the tetrahydrofuran ring (7-*O*-8′). The NOESY correlations between H-7′ and H-7, and between H-7 and H-9 suggested that H-7, H-7′, and $H_3$-9 were on the same face of the tetrahydrofuran ring adopting the opposite orientation as H-8. Therefore, the relative configuration of **2** was designated as 7*R**, 8*R**, 7′*S**, 8′*R**, and named as magnosalicin [12]. In addition, the four related known compounds, including (±) acoraminol A (**3**) [10], (±) acoraminol B (**4**) [10], asaraldehyde (**5**) [10], 2, 4, 5-trimethoxybenzoic acid (**6**) [13] were determined by detailed analyses of HR-ESIMS, NMR data, and comparison of the NMR data with reported values.

However, the optical rotations of **1** and **2** were closed to zero, indicating that **1** and **2** might be present as racemic manners, which were confirmed by the presence of two peaks in chiral HPLC. Then, two pairs of enantiomers **1a** [$t_R$ 16.5 min $[\alpha]_D^{27}$ +52.8 (*c* 1.00, MeOH)]/**1b** [$t_R$ 18.5 min $[\alpha]_D^{27}$ −58.0 (*c* 1.00, MeOH)] and **2a** [$t_R$ 15.5 min $[\alpha]_D^{27}$ +104.0 (*c* 0.25, MeOH)]/**2b** [$t_R$ 19.5 min $[\alpha]_D^{27}$ −124.0 (*c* 0.25, MeOH)] were separated by using a Phenomenex Lux™ Amylose-2 column (5 μm, 250 mm × 4.6 mm) with $CH_3CN$−$H_2O$ (40 : 60, *V*/*V*) and $CH_3CN$−$H_2O$ (45 : 55, *V*/*V*) at a flow rate of 1 mL·min$^{-1}$, respectively (Fig. 4). Moreover, the quantum chemical ECD calculations were used to determine the absolute configurations of **1a** and **1b**. As the methoxy group in **1a** and **1b** had an insignificant effect on the ECD spectrum [10], the simplified structures of (7*R*, 8*R*, 7′*R*, 8′*S*)-**1′** and (7*S*, 8*S*, 7′*S*, 8′*R*)-**1′** were used for ECD calculations at the B3LYP/TZVP level. The predicted ECD curves of (7*R*, 8*R*, 7′*R*, 8′*S*)-**1′** and (7*S*, 8*S*, 7′*S*, 8′*R*)-**1′** were almost identical to the experimental ones of **1b** and **1a**, respectively (Fig. 5). Therefore, the absolute configurations of **1a** and **1b** were established as (7*S*, 8*S*, 7′*S*, 8′*R*)-**1a** and (7*R*, 8*R*, 7′*R*, 8′*S*)-**1b**, respectively. Similarly, the absolute configurations of **2a** (7*R*, 8*R*, 7′*S*, 8′*R*) and **2b** (7*S*, 8*S*, 7′*R*, 8′*S*) were determined by ECD calculations at the wb97XD/TZVP level, respectively (Fig. 6). Furthermore, the single-crystal X-ray crystallographic analysis of **1b** (Fig. 7) confirmed the above deduction, and the values of the Flack parameter [0.07(14)] and the Hooft parameter [0.04(7)] allowed to establish the absolute configuration of **1b** as 7*R*, 8*R*, 7′*R*, 8′*S*.

All the compounds were evaluated for their cytotoxicities against five human tumor cell lines (SW480, MCF-7, A-549, SMMC-7721, and HL-60) and anti-A$\beta_{42}$ aggregation

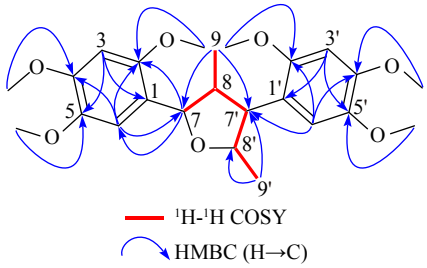


**Fig. 2 Key $^1$H−$^1$H COSY and HMBC correlations for 1**

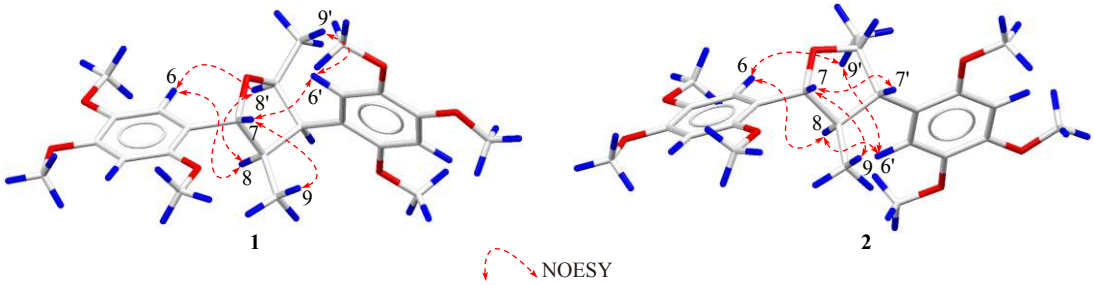


**Fig. 3 Key NOESY correlations for 1–2**

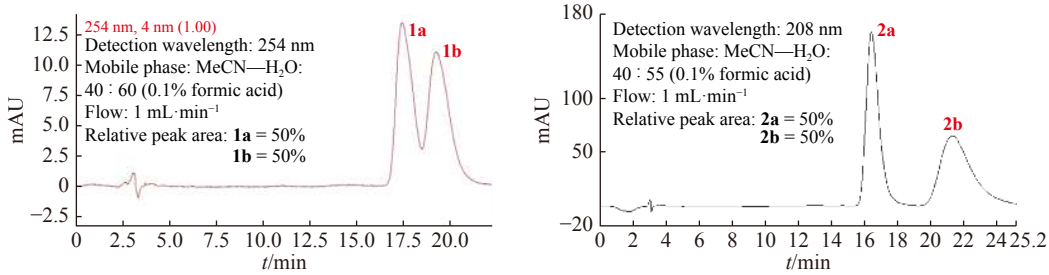


**Fig. 4 The chiral HPLC chromatograms of 1–2**

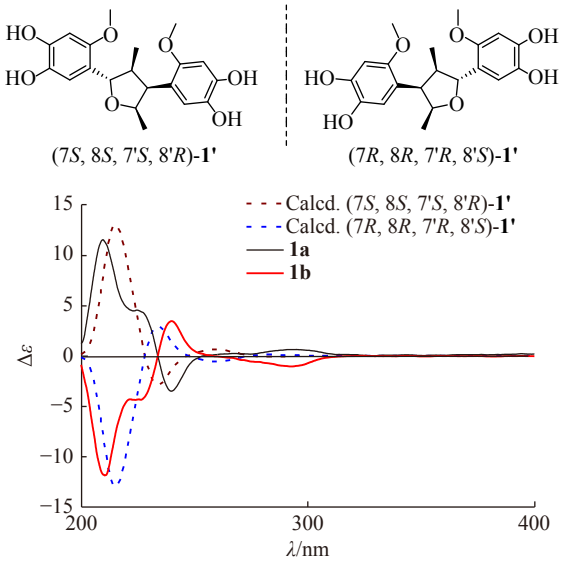


**Fig. 5 Experimental ECD spectra of 1a and 1b, and calculated ECD spectra of (7*R*, 8*R*, 7′*R*, 8′*S*)-1′ and (7*S*, 8*S*, 7′*S*, 8′*R*)–1′ (UV correction = 0 nm, band width *σ* = 0.20 eV)**

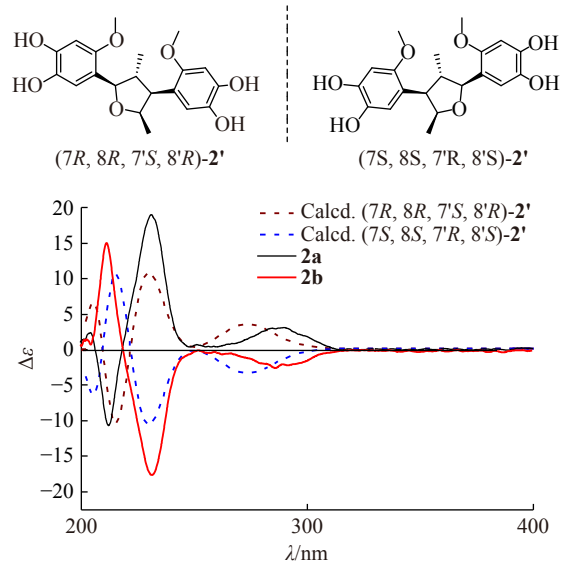


**Fig. 6 Experimental ECD spectra of 2a and 2b, and calculated ECD spectra of (7*R*, 8*R*, 7′*S*, 8′*R*)-2′ and (7*S*, 8*S*, 7′*R*, 8′*S*)–2′ (UV correction = +15 nm, band width σ = 0.30 eV)**

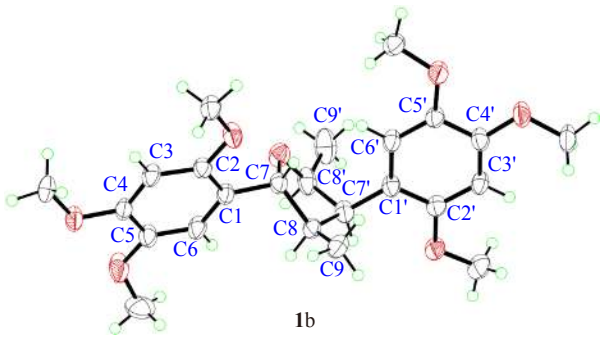


**Fig. 7 X-ray structure of 1b**

activities. The results showed that none of the compounds possessed cytotoxic activities, while compound **2** exhibited significant anti-A$\beta_{42}$ aggregation activity with an inhibitory rate of 60.81%, in constrast to 69.17% for the positive control EGCG.

The biotransformation pathway of *α*-asarone by *Alternaria longipes* CGMCC 3.2875 was proposed (Scheme 1). The formation of **1**–**4** was likely to initiate with oxidation of the 7, 8-double bond of *α*-asarone to give intermediate **a**. Then, the subsequent dimerization afforded **1** and **2** [12], while direct oxidation of intermediate **a** followed by methoxylation afforded **3** and **4**. Compounds **5**–**6** were generated by oxidative cleavage at the 7, 8-double bond of *α*-asarone.

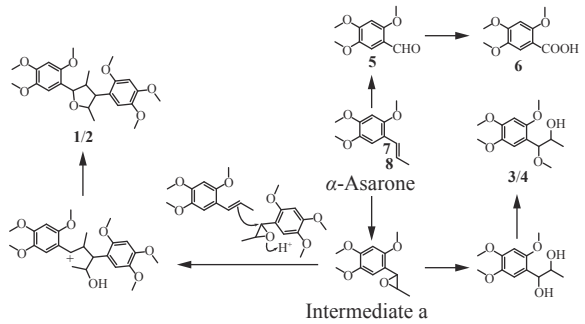


**Scheme 1 Proposed pathway of *α*-asarone metabolized by *Alternaria longipes* CGMCC 3.2875**

## Conclusion

In summary, microbial transformation of *α*-asarone by *Alternaria longipes* CGMCC 3.2875 leads to the isolation of two pairs of new rare neolignans, (+) (7*S*, 8*S*, 7′*S*, 8′*R*) *iso*-magnosalicin (**1a**)/(−) (7*R*, 8*R*, 7′*R*, 8′*S*) *iso*-magnosalicin (**1b**) and (+) (7*R*, 8*R*, 7′*S*, 8′*R*) magnosalicin (**2a**)/(−) (7*S*, 8*S*, 7′*R*, 8′*S*) magnosalicin (**2b**), and four known metabolites (**3**–**6**). This is the first time to obtain optically pure magnosalicin type neolignans and establish their absolute configurations. Among them, the magnosalicin (**2**) shows anti-A$\beta_{42}$ aggregation activity. The results suggest that the biotransformation is a practical approach to generate the new bioactive derivatives of *α*-asarone and establish the material foundation for future metabolic studies of *α*-asarone.

## Experimental

### *General experimental procedures*

Methanol (MeOH) was purchased from Yuwang Industrial Co., Ltd. (Yucheng, China). Acetonitrile (MeCN) was obtained from Oceanpak Alexative Chemical Co., Ltd. (Gothenburg, Sweden). Ethyl acetate (EtOAc) was purchased from Fine Chemical Co., Ltd. (Tianjin, China).

The melting points were determined on an X-5 micro-melting point apparatus (Beijing TECH Instrument Co., Ltd., Beijing, China) without correction. X-ray data was collected at 100 K on a Rigaku Oxford Diffraction Supernova Dual Source (Agilent Technologies Inc., California, USA). Optical rotation values were measured on a JASCO P1020 digital polarimeter (Jasco International Co., Ltd., Tokyo, Japan), and UV data were recorded on a JASCO V-550 UV/vis spectrometer (Jasco International Co., Ltd, Tokyo, Japan). ECD

spectra were recorded on a JASCO J-810 spectrophotometer (Jasco International Co., Ltd., Tokyo, Japan) using MeOH as the solvent. IR data were recorded using a JASCO FT/IR-480 plus spectrometer (Jasco International Co., Ltd., Tokyo, Japan). HR-ESI-MS spectra were obtained on Waters Synapt G2 mass spectrometer (Waters Co., Milford, America). $^{1}$H and $^{13}$C NMR spectra were obtained with Bruker AV 400/AV 300 (Bruker BioSpin Group, Faellanden, Switzerland) using solvent signal ($CD_3OD$: $\delta_H$ 3.30/$\delta_C$ 49.0, $CDCl_3$: $\delta_H$ 7.26/$\delta_C$ 77.0) as an internal standard. Analytical HPLC was performed on a Shimadzu HPLC (Shimadzu Co., Ltd., Kyoto, Japan) system equipped with an LC-20AB pump, an SPD-M20A diode array detector, a SIL-20A autosampler using a YMC-C18 column (4.6 mm × 250 mm, 5 μm, YMC Co., Ltd., Kyoto, Japan) and a Phenomenex Lux™ Amylose-2 column (4.6 mm × 250 mm, 5 μm, Phenomenex Co., Ltd., Torrance, CA, USA). Semi-preparative HPLC was carried out on a Shimadzu LC-6AD (Shimadzu Co., Ltd., Kyoto, Japan) system equipped with a UV detector using a YMC-$C_{18}$ column (10.0 mm × 250 mm, 5 μm, YMC Co., Ltd., Kyoto, Japan). Column chromatography (CC) was carried out on ODS (50 μm, YMC Co., Ltd., Kyoto, Japan). TLC was performed on a precoated silica gel plate (SGF254, 0.2 mm, Yantai Chemical Industry Research Institute, Yantai, China).

*Substrate*

The substrate *α*-asarone (with purity > 98%) was isolated from *Acorus tatarinowii* Schott. Its structure was characterized by $^{1}$H and $^{13}$C NMR data compared with previous reports [14].

*Microorganism and culture medium*

All 24 microorganism strains were obtained from Professor QIU Feng in Tianjin University of Traditional Chinese Medicine (Tianjin, China). These strains used for preliminarily screening the biotransformation of *α*-asarone were listed as follows: *Absidia coerulea* CGMCC 3.3389, *Alternaria alternata* CGMCC 3.4578, *Alternaria longipes* CGMCC 3.2875, *Aspergillus cabonarius* CICC 2087, *Aspergillus flavus* CGMCC 3.3554, *Aspergillus fumigatus* CICC 2168, *Aspergillus niger* CGMCC 3.1858, *Aspergillus niger* CGMCC 3.739, *Aspergillus niger* CGMCC 3.795, *Cunninghamella blakesleana* CGMCC 3.970, *Cunninghamella elegans* CGMCC 3.1207, *Fusarium avenaceum* CGMCC 3.4594, *Mucor polymorphosporus* CGMCC 3.3443, *Mucor spinosus* CICC 40243, *Mucor subtilissimus* CGMCC 3.2454, *Paecilomyces variotii* CICC 4024, *Penicillium adametzii* CGMCC 3.4470, *Penicillium citrinum* CICC 4013, *Penicillium decumbens* CGMCC 3.5255, *Penicillium janthinellum* CGMCC 3.514, *Penicillium melinii* CGMCC 3.4474, *Penicillium urticae* CICC 4015, *Sporotrichum* sp. CGMCC 3.2882, and *Syncephalastrum racemosum* CGMCC 3.264. Stock cultures were maintained at 4 °C on agar slants containing PDA in an Eyela LTI-700 conventional incubator (Tokyo Rikakikai Co., Ltd., Tokyo, Japan). All initial screening experiments were performed in conical flasks (500 mL) containing 100 mL of PDB, which was sterilized by autoclaving at 121 °C for 30 min using an MLS3750 autoclave (Sanyo Electric Co., Ltd., Moriguchi, Japan).

*Biotransformation of α-asarone and isolation of metabolites*

The preparative scale biotransformation of *α*-asarone by *Alternaria longipes* CGMCC 3.2875 was carried out in 22 (3000 mL) flasks each containing 500 mL of medium. After incubation for five days, the cultures were incubated for 72 h before addition of 3.3 g of substrate in total (dissolved in methanol). The incubation conditions and extraction procedures were the same with those described in preliminary screening experiment. The crude extract 7.8 g was subjected to an open ODS chromatography column eluted with MeOH−$H_2O$ (20 : 80, 40 : 60, 60 : 40, 80 : 20, and 100 : 0, *V/V*) to produce 10 fractions (E1 to E10). E3 (65.68 mg) was purified on semi-preparative HPLC (MeOH−$H_2O$, 35 : 65, 0.1% formic acid; 3.0 mL·min$^{-1}$, 254 nm) to produce **6** ($t_R$ 10.5 min, 15.7 mg). E4 (80.22 mg) was purified on semi-preparative HPLC ($CH_3CN$−$H_2O$, 40 : 60, 3.0 mL·min$^{-1}$, 254 nm) to produce **5** ($t_R$ 11.2 min, 6.5 mg), **4** ($t_R$ 19.5 min, 2.0 mg), and **3** ($t_R$ 21.5 min, 4.1 mg). E7 (357.39 mg) was purified on semi-preparative HPLC ($CH_3CN$−$H_2O$, 50 : 50, 3.0 mL·min$^{-1}$, 254 nm) to produce **2** ($t_R$ 17.5 min, 7.8 mg), and **1** ($t_R$ 20.5 min, 5.4 mg). **1** was further separated by a Phenomenex Lux™ Amylose-2 column (250 mm × 4.6 mm, 5 μm, $CH_3CN$−$H_2O$ 40 : 60 with 0.1% formic acid, 1 mL·min$^{-1}$) to generate **1a** ($t_R$ 16.5 min, 1.5 mg) and **1b** ($t_R$ 18.5 min, 1.2 mg). **2** was further separated by a Phenomenex Lux™ Amylose-2 column (250 mm × 4.6 mm, 5 μm, $CH_3CN$−$H_2O$ 45 : 55 with 0.1% formic acid, 1 mL·min$^{-1}$) to produce **2a** ($t_R$ 15.5 min, 2.5 mg) and **2b** ($t_R$ 19.5 min, 2.2 mg).

*iso-Magnosalicin (**1**)*

$C_{24}H_{32}O_7$, white powder; UV (MeOH) $\lambda_{max}$ (log $\varepsilon$): 206 (4.70), 233 (4.21), 293 (3.95) nm; IR (KBr) $\nu_{max}$: 2931, 1615, 1511, 1319, 1209, 1034 cm$^{-1}$; HR-ESIMS (positive): *m/z* 455.2046 $[M + Na]^+$ (Calcd. for $C_{24}H_{32}O_7Na$, *m/z* 455.2039). For $^{1}$H (400 MHz, $CD_3OD$) and $^{13}$C (100 MHz, $CD_3OD$) NMR data see Tables 1−2.

(+) (7*S*, 8*S*, 7′*S*, 8′*R*) *iso*-Magnosalicin (**1a**): white powder; $[\alpha]_D^{27}$ +52.8 (*c* 1.0, MeOH); ECD (6.8 × 10$^{-5}$ mol·L$^{-1}$, MeOH) $\lambda_{max}$ ($\Delta\varepsilon$): 210 (+17.06), 230 (+4.67), 235 (−1.72), 290 (+0.83) nm.

(−) (7*R*, 8*R*, 7′*R*, 8′*S*) *iso*-Magnosalicin (**1b**): colorless block-shaped crystals (MeOH); mp 138.2−140.5 °C; $[\alpha]_D^{27}$ −58.0 (*c* 1.0, MeOH); ECD (11.1 × 10$^{-5}$ mol·L$^{-1}$, MeOH) $\lambda_{max}$ ($\Delta\varepsilon$): 210 (−11.85), 230 (−3.20), 235 (+1.13), 290 (−1.06) nm.

*Magnosalicin (**2**)*

$C_{24}H_{32}O_7$, white powder; UV (MeOH) $\lambda_{max}$: (log $\varepsilon$) 205 (4.78), 232 (4.29), 291 (4.02) nm; IR (KBr) $\nu_{max}$: 2926, 1605, 1517, 1322, 1208, 1031 cm$^{-1}$; HR-ESIMS (positive): *m/z* 455.2044 $[M + Na]^+$ (Calcd. for $C_{24}H_{32}O_7Na$, *m/z* 455.2046). For $^{1}$H (300 MHz, $CDCl_3$) and $^{13}$C (75 MHz, $CDCl_3$) NMR data see Tables 1−2.

(+) (7*R*, 8*R*, 7′*S*, 8′*R*) Magnosalicin (**2a**): white powder; $[\alpha]_D^{27}$ +104.0 (*c* 0.25, MeOH); ECD (11.6 × 10$^{-5}$ mol·L$^{-1}$, MeOH) $\lambda_{max}$ ($\Delta\varepsilon$): 212 (−10.60), 230 (+18.67), 254 (+0.60), 288 (+2.84) nm.

(−) (7*S*, 8*S*, 7′*R*, 8′*S*) Magnosalicin (**2b**): white powder; $[\alpha]_D^{27}$ −124.0 (*c* 0.25, MeOH); ECD (11.6 × 10$^{-5}$ mol·L$^{-1}$, MeOH) $\lambda_{max}$ ($\Delta\varepsilon$): 212 (+14.71), 230 (−17.34), 235 (−0.45), 288 (−2.43) nm.

*X-ray crystallographic analysis of **1b***

Upon crystallization from MeOH using the vapor diffu-

sion method, colorless block-shaped crystals of **1b** were obtained. Data were collected by a Sapphire CCD with graphite monochromated Cu K$\alpha$ radiation, $\lambda$ = 1.54184 Å at 173.0 (4) K. Crystal data: $C_{24}H_{32}O_7$, $M$ = 432.50, space group monoclinic, $P$ $2_1$; unit cell dimensions were determined to be $a$ = 7.5211 (2) Å, $b$ = 17.4868 (4) Å, $c$ = 8.7933 (2) Å, $\alpha$ = 90.00°, $\beta$ = 102.441 (3)°, $\gamma$ = 90.00°, $V$ = 1129.34 (5) Å$^3$, $Z$ = 2, $Dx$ = 1.272 mg·m$^{-3}$, $F$ (000) = 464, $\mu$ (Cu K$\alpha$) = 0.763 mm$^{-1}$. 15 059 reflections were collected to $\theta_{max}$ = 62.81°, in which 3618 independent unique reflections ($R_{int}$ = 0.0334, $R_{sigma}$ = 0.0232) were used in all calculations. Using Olex2 [15] (Olex2 version, OlexSys Ltd., Durhum, England), the structure was solved by direct methods using the SHELXS program, and refined by the SHELXL program and full-matrix least-squares calculations. During structure refinement, hydrogen atoms were placed on the geometrically ideal positions by the "ride on" method. The final refinement gave $R_1$ = 0.0292 (I > 2σ(I)), w$R_2$ = 0.0757 (all data), $S$ = 1.056, Flack = 0.07 (14), and Hooft = 0.04 (7). Crystallographic data for **1b** were deposited in the Cambridge Crystallographic Data Center with supplementary publication no. CCDC 2083899. The copies of these data are freely available, on request to the Director, CCDC, 12 Union Road, Cambridge CB2 1EZ, UK (Fax: +44-(0)1223-336033, or E-mail: deposit@ccdc.cam.ac.uk).

*Cytotoxicity assay*

The cytotoxicity assay was performed using the 3-(4, 5-dimethylthiazol-2-yl)-5-(3-carboxymethoxyphenyl)-2-(4-sulfophenyl)-2*H*-tetrazolium (MTS) assay [16]. Five human cancer cell lines (human colon cancer SW480, human breast cancer MCF-7, human lung cancer A-549, human hepatocarcinoma SMMC-7721, and human promyelocytic leukemia HL-60) were used for the cytotoxicity assay. All the cells were cultured in DMEM medium supplemented with 10% fetal bovine serum at 37 °C in an atmosphere of 5% $CO_2$. Briefly, 1 × 10$^4$ cells were seeded into each well of 96 well plates and treated with 40 μM of the corresponding compounds for 48 h, with cisplatin and taxol as the positive control. Then, 20 μL aliquot of 0.5% MTS (Sigma, USA) solution was added to each well, following by incubation for 4 h. Then, the culture medium was removed, and the resultant formazan precipitates were dissolved with 150 μL of DMSO. The absorbance (Ab) of the samples was measured at 490 nm using a microtiter plate reader. The cell viability of each compound was calculated by the following formula: $[(Ab_{sample} - Ab_{blank})/(Ab_{DMSO} - Ab_{blank})] \times 100\%$.

*ThT fluorescence assay*

The protocol for standard thioflavin T (ThT) fluorescence assay was performed according to previous studies [17-18]. The fluorescence reached 300 min (Ex 444 nm; Em 485 nm) in a microplate reader (Fluoroskan Ascent, Thermo Scientific, USA). The bioactivities were indicated by relative inhibit rate ($V_i$) according to the formula: $V_i = 100 - [(F_i - F_b)/F_0] \times 100$, where $F_i$ is the fluorescence value of the sample groups (containing sample, A$\beta_{42}$ and ThT), $F_b$ is its blank value (containing sample and ThT), and $F_0$ is the fluorescence valueforfreeaggregationofA$\beta_{42}$incubatedinthesamebuffer/HFIP/DMSO system (containing A$\beta_{42}$ and ThT). The inhibitory rate (%) was calculated from the mean of seven different independent experiments with standard errors.

## References


[1] Liu JH, Yu BY. Biotransformation of bioactive natural products for pharmaceutical lead compounds [J]. *Curr Org Chem*, 2010, **14**(14): 1400-1406.

[2] Rocha BA, Assis MD, Peti AP, *et al*. *In vitro* metabolism of monensin A: microbial and human liver microsomes models [J]. *Xenobiotica*, 2014, **44**(4): 326-335.

[3] Zhong JC, Li XB, Lyu WY, *et al*. Natural products as potent inhibitors of hypoxia-inducible factor-1$\alpha$ in cancer therapy [J]. *Chin J Nat Med*, 2020, **18**(9): 696-703.

[4] Fan HX, Zhou ZQ, Peng J, *et al*. A microbial model of mammalian metabolism: biotransformation of 4, 5-dimethoxylcanthin-6-one using *Cunninghamella blakesleeana* CGMCC 3.970 [J]. *Xenobiotica*, 2017, **47**(4): 284-289.

[5] Feng XL, Yu Y, Qin DP, *et al*. *Acorus linnaeus*: a review of traditional uses, phytochemistry and neuropharmacology [J]. *RSC Adv*, 2015, **5**(7): 5173-5182.

[6] Chellian R, Pandy V, Mohamed Z, *et al*. Pharmacology and toxicology of $\alpha$- and $\beta$-Asarone: a review of preclinical evidence [J]. *Phytomedicine*, 2017, **32**: 41-58.

[7] Feng XL, Yu Y, Gao H, *et al*. New sesquiterpenoids from the rhizomes of *Acorus tatarinowii* [J]. *RSC Adv*, 2014, **4**(79): 42071-42077.

[8] Qin DP, Feng XL, Zhang WY, *et al*. Anti-neuroinflammatory asarone derivatives from the rhizomes of *Acorus tatarinowii* [J]. *RSC Adv*, 2017, **7**(14): 8512-8520.

[9] Zhang WY, Feng XL, Lu D, *et al*. New lignans attenuating cognitive deterioration of A$\beta$ transgenic flies discovered in *Acorus tatarinowii* [J]. *Bioorg Med Chem Lett*, 2018, **28**(4): 814-819.

[10] Gao E, Zhou ZQ, Zou J, *et al*. Bioactive asarone-derived phenylpropanoids from the rhizome of *Acorus tatarinowii* Schott [J]. *J Nat Prod*, 2017, **80**(11): 2923-2929.

[11] Gao E, Ren FF, Zou J, *et al*. Chiral resolution, absolute configuration, and bioactivity of a new racemic asarone derivative from the rhizome of *Acorus tatarinowii* [J]. *Fitoterapia*, 2017, **122**: 7-10.

[12] Tsuruga T, Ebizuka Y, Nakajima J, *et al*. Biologically active constituents of *Magnolia salicifolia*: inhibitors of induced histamine release from rat mast cells [J]. *Chem Pharm Bull (Tokyo)*, 1991, **39**(12): 3265-3271.

[13] Evans JC, Klix RC, Bach RD. Diels-Alder approaches to model compounds related to fredericamycin A [J]. *J Org Chem*, 1988, **53**(23): 5519-5527.

[14] Joshi BP, Sharma A, Sinha AK. Ultrasound-assisted convenient synthesis of hypolipidemic active natural methoxylated (*E*)-arylalkenes and arylalkanones [J]. *Tetrahedron*, 2005, **61**(12): 3075-3080.

[15] Dolomanov OV, Bourhis LJ, Gildea RJ, *et al*. OLEX2: a complete structure solution, refinement and analysis program [J]. *J Appl Crystallogr*, 2009, **42**(2): 339-341.

[16] Yang YF, Liu JQ, Li ZR, *et al*. New eudesmenoic acid methyl esters from the seed oil of *Jatropha curcas* [J]. *Fitoterapia*, 2013, **89**: 278-284.

[17] Zhao H, Wang GQ, Tong XP, *et al*. Diphenyl ethers from *Aspergillus* sp. and their anti-A$\beta_{42}$ aggregation activities [J]. *Fitoterapia*, 2014, **98**: 77-83.

[18] Chakrabortee S, Liu Y, Zhang L, *et al*. Macromolecular and small-molecule modulation of intracellular A$\beta_{42}$ aggregation and associated toxicity [J]. *Biochem J*, 2012, **442**(3): 507-515.


**Cite this article as:** ZOU Jian, ZHANG Shuai, ZHAO Huan, WANG Yong-Heng, ZHOU Zheng-Qun, CHEN Guo-Dong, HU Dan, LI Ning, YAO Xin-Sheng, GAO Hao. Biotransformation of $\alpha$-asarone by *Alternaria longipes* CGMCC 3.2875 [J]. *Chin J Nat Med*, 2021, **19**(9): 700-705.